Supplementary Materials for

CD47-SIRPα axis blockade in NASH promotes necroptotic hepatocyte clearance by liver macrophages and decreases hepatic fibrosis

Hongxue Shi *et al.*

Corresponding authors. Hongxue Shi, hs3205@columbia.edu;and Ira Tabas, iat1@columbia.edu

The PDF file includes:

Materials and Methods

Figs. S1 to S8

Tables S1 to S2

References (63-72)

Other Supplementary Material for this manuscript includes the following:

MDAR Reproducibility Checklist

SUPPLEMENTARY MATERIALS

MATERIALS AND METHODS

Liver histology staining and plasma ALT measurement

Livers were fixed in 10% formalin for at least 24 hours before paraffin embedding and then sectioned for histological analysis, including hematoxylin and eosin (HE) staining, Picrosirius Red staining (Polysciences, #24901), and trichrome staining (Sigma, #HT15), according to the manufacturer's protocol. Plasma alanine transaminase (ALT) activity was measured using a commercial kit (Teco Diagnostics, #A526). NAS score (*63*) was calculated based on hepatocyte steatosis (0, <5%; 1, 5%–33%; 2, 34%–66%; 3, >66%) and lobular inflammation (0, none; 1, <2 foci per 200× field; 2, 2–4 foci per 200× field; 3, >4 foci per 200× field); we did not observe hepatocyte ballooning, which is consistent with previous findings (*64*).

Liver primary cell isolation

The methods for isolating primary hepatocytes and resident Kupffer cell (KCs) were published as described previously (*34, 65*). Briefly, livers of male C57BL/6J mice were perfused with HBSS perfusion buffer (Corning, #21-022-CV) containing HEPES (Sigma, #H0887, 25 mM) and EDTA (Invitrogen, #15575-038, 0.5 mM) and then with HBSS digestion buffer (Gibco, #14025-092) containing collagenase D (4.4 U/mouse, Roche, #11088882001). The digested livers were gently ruptured to release cells, and suspended cells were centrifuged at 50 *g* for 1 min at 4 °C to pellet hepatocytes. The hepatocytes were plated on collagen-coated culture dishes in DMEM/F12 medium with 10% FBS and 1% penicillin-streptomycin. Next, the supernate fractions from the 50 *g* spin were used for KC isolation: the fractions were centrifuged at 50 *g* for 1 min to remove any residual hepatocytes, and then non-parenchymal cells were pelleted. KCs were isolated with anti-F4/80 beads (Miltenyi Biotec, #130-110-443) and cultured in DMEM medium containing 10% FBS and 1% penicillin-streptomycin. Primary human Kupffer cells (#HK1000.H15) and hepatocytes (#H1000.H15-3) were obtained from Sekisui XenoTech Company.

Ex vivo efferocytosis assay

KCs were seeded in 8-well chamber slide and cultured at 37°C overnight. To generate necroptotic mouse hepatocytes, hepatocytes were isolated from mice that had been injected with AAV8-TBG-mRIP3-2xFV, and the hepatocytes were treated ex vivo with 10 nM AP20187 for 6 hours. Human hepatocytes were infected with retrovirus expressing 2xFV-hRIP3 (*66*) to generate necHCs which were then labeled with PKH67 (Sigma, #MINI67) according to the manufacturer's protocol. To induce apoptosis in mouse hepatocytes, mice were given Fas ligand (Jo2, BD Biosciences, # 554254, RRID:AB_395326, 100 μg/kg) via intravenous injection and then hepatocytes were isolated and cultured for 6 hours. In experiments involving anti-CD47, necHCs were pre-treated with 20 μg/ml anti-CD47 antibody (Bio-X-Cell, #BE0283, RRID:AB_2687806) or IgG control for 30 min and then incubated with KCs for 6 hours. For the anti-SIRPα experiments, necHCs were incubated with 20 μg/ml anti-SIRPα (Bio-X-Cell, #BE0322, RRID:AB_2819049) or IgG control and then incubated with KCs for 6 hours. The KCs then were fixed in 4% paraformaldehyde, and F-actin was labeled with phalloidin-iFluor 594 reagent (Abcam, #ab176757). Images were taken using a green spinning-disk confocal microscope (Nikon Ti), and the data were analyzed using Imaris 9.5 quantification software.

Immunohistochemistry staining

Liver paraffin sections were deparaffinized and hydrated and then subjected to antigen retrieval using citrate sodium (Vector laboratory, #H-3300) in a high-pressure cooker. Next, the sections were incubated with 3% H2O2 for 10 min at room temperature to block endogenous peroxidase activity, blocked with 5% donkey serum for 1 hour at room temperature, and incubated with anti-mouse p-MLKL (Cell signaling technology, #37333S, RRID:AB_2799112, 1:100 dilution), Col1a1 (Cell signaling technology, #72026S, RRID:AB_2904565, 1:200 dilution) or anti-Mac 2 (Cedarlane, # CL8942AP, RRID:AB_10060357, 1:1000 dilution) in 1% donkey serum at 4 °C overnight. The sections were then incubated with SignalStain boost IHC detection reagent from Cell Signaling Technology (HRP, Rabbit, #8114; HRP, Rat, #72838; AP, Rabbit, #18653), followed by color development using a DAB substrate kit (Cell signaling technology, #8059) or SignalStain Vibrant Red Alkaline

Phosphatase Substrate kit (Cell signaling technology, #76713). Finally, the liver sections were counterstained with hematoxylin, dehydrated, and mounted. The images were taken using a Nikon microscope, and the data were analyzed using Image J software.

Immunofluorescence staining and in-situ phagocytosis assay

Liver paraffin sections were deparaffinized, hydrated, and blocked with 5% donkey serum. For immunofluorescence experiments, human liver sections were incubated with anti-human p-MLKL (Cell Signaling Technology, #91689, RRID:AB_2732034, 1:100 dilution), RIP3 (ProSci, #2283, RRID:AB_203256, 1:100 dilution), CD47 (Santa Cruz, # SC-12730, RRID:AB_627086, 1:100 dilution), CD68 (Agilent, #GA60961-2, RRID:AB_2661840, 1:500 dilution or Cell Signaling Technology, #76437s, RRID:AB_2799882, 1:200), SIRPα (Cell Signaling Technology, #13379s, RRID:AB_2798196, 1:200 dilution) and Hep par1 (Abcam, ab234028, 1:100 dilution) in 1% donkey serum at 4 °C overnight; mouse liver sections were incubated with anti-Mac2 (Cedarlane, #CL8942AP, RRID:AB_10060357, 1:500 dilution), anti-Clec4f (RD, #AF2784, RRID:AB_2081339, 1:200 dilution), anti-F4/80 (Cell Signaling Technology, #70076s, RRID:AB_2799771, 1:200), anti-osteopontin (Opn, RD, #AF808, RRID:AB_2194992, 1:100 dilution), and/or anti-SIRPα (Cell Signaling Technology, #13379s, RRID:AB_2798196, 1:200 dilution) in 1% donkey serum at 4 °C overnight Fluorescent dye-conjugated secondary antibodies were used (1:250 dilution) for 1 hour at room temperature, followed by nuclei staining with DAPI. For the in-situ phagocytosis assessment, mouse liver sections were incubated with the pan-macrophage marker anti-Mac2 (Cedarlane, #CL8942AP, RRID:AB_10060357, 1:500 dilution) or the KC marker anti-Clec4f (RD, #AF2784, RRID:AB_2081339, 1:200 dilution) and the necroptosis marker RIP3 (Enzo, #ADI-905-242-100, RRID:AB_2039527, 1:200 dilution) in 1% donkey serum at 4 °C overnight, followed by fluorescent dye-conjugated secondary antibodies administration. The ratio of macrophage-internalized to total $RIP3^+$ cells was quantified as a measure of the efficiency of macrophage-mediated clearance of necHCs. The images were captured using a Leica DMI 6000B fluorescence microscope, and the data were analyzed using Image J software. For RIP3 and CD47 immunofluorescence co-staining experiment, 100-μm liver

sections were permeabilized with PBS containing 1% Triton X-100 for 2 hours at room temperature and blocked with 1% donkey serum in PBS containing 0.1% Triton X-100 for overnight at 4 °C. Primary anti-mouse antibodies against RIP3 (Enzo, #ADI-905-242-100, RRID:AB_2039527, 1:200 dilution) and CD47 (BD, #555297, RRID:AB_395713, 1:100 dilution) were applied to liver sections in PBS with 1% donkey serum for 2 days at 4 °C. The liver sections were incubated with fluorescent-dye conjugated secondary antibodies overnight at 4 °C. Cellular nuclei were stained with DAPI, and images were taken using a green-spinning disk confocal microscope (Nikon, Ti). The image data analysis was performed using Image J software.

Immunoblotting

Liver protein was extracted using RIPA lysis buffer (Thermo, #89901) with a proteinase and phosphatase inhibitor cocktail (Thermo, #78445), followed by protein concentration measurement using a BCA kit (Thermo, #23227). To isolate insoluble MLKL from mouse liver, the extract was pelleted at 15000 *g* for 20 min at 4°C and then resuspended by sonication in RIPA buffer containing 8 M urea, as described (*19*). 20 µg total protein was separated on 4-20% Tris-gels (Life technologies, EC60285) and transferred to nitrocellulose membranes (Bio-Rad, #1620115). The membranes were blocked with 5% non-fat milk in Tris-buffered saline with 0.1% Tween 20 (TBST) for 1 hour at room temperature, The membranes were then incubated with antibodies recognizing human p-MLKL (Cell Signaling Technology, #91689, RRID:AB_2732034, 1:1000 dilution) and total MLKL (Cell signaling technology, #14993, RRID:AB_2721822, 1:1000 dilution), RIP3 (ProSci, # 2283, RRID:AB_203256, 1:1000 dilution), or CD47 (Thermo, #14-0479-82, RRID:AB_837143, 1:1000 dilution), SIRPα (Cell Signaling Technology, #13379s, RRID:AB_2798196, 1:1000 dilution); or with antibodies against mouse MLKL (Millipore, #MABC604, RRID:AB_2820284, 1:1000 dilution) , RIP3 (Cell signaling technology, #15828, RRID:AB_2722663, 1:1000 dilution), or SIRPα (Cell Signaling Technology, #13379s, RRID:AB_2798196, 1:1000 dilution) overnight at 4°C. The membranes were then incubated with HRP-conjugated second antibodies (Jackson ImmunoResearch , #711-035-152, RRID:AB_10015282, 1:5000 dilution) for 1 hour at room temperature, and bands were detected with SuperSignal West Pico PLUS Chemiluminescent Substrate (Thermo, # 34580).

Quantitative RT-qPCR

Total liver mRNA was extracted using TRIzol Reagent (Thermo, #15596026) and purified using Purelink RNA mini kit (Thermo, #12183025). The mRNA concentration was measured using nano-drop spectrophotometers, and 1 µg total mRNA was used to synthesize cDNA using high-capacity cDNA reverse transcription kit (Applied Biosystems, #4368813). mRNA expression levels were measured with a 7500 Real-time PCR system (Applied Biosystems) using SYBR green dye (Life Technologies, #4367659). Primer sequences are listed in **table S2**.

RNA-seq in liver and data analysis

Total mRNA was extracted from anti-CD47 or IgG treated mice liver tissues using RNeasy Mini Kit (Qiagen, #74104). The libraries were constructed using Illumina TruSeq chemistry and then sequenced using Illumina NovaSeq 6000 at the Columbia Genome Center. For data analysis, FASTQ files were quantified with Salmon v1.3.0 to obtain transcript abundance counts using an index made from GRCm39 GENCODE VM27 (*67*). The resulting counts were summarized to the gene level using tximport v1.20.0 (*68*). Differential expression was assessed using DESeq2 v1.32.0 (*69*). Genes with an absolute fold change > 1.5 and false discovery rate (FDR)-adjusted P value < 0.05 were considered as differentially expressed (DE). The output of DESeq2 was scored and ranked by apeglm (*70*) using ranking metrics "−log10 P value multiplied by the sign of log-transformed fold-change" (*71*). The ranked gene list was then used for Gene Set Enrichment Analysis (GSEA) (*72*) to identify the gene sets overrepresented at the top or bottom of the ranked list using pathway definition files downloaded from http://baderlab.org/GeneSets as described (*71*). The leading-edge genes enriched in the identified pathways were visualized by using pheatmap v1.0.12.

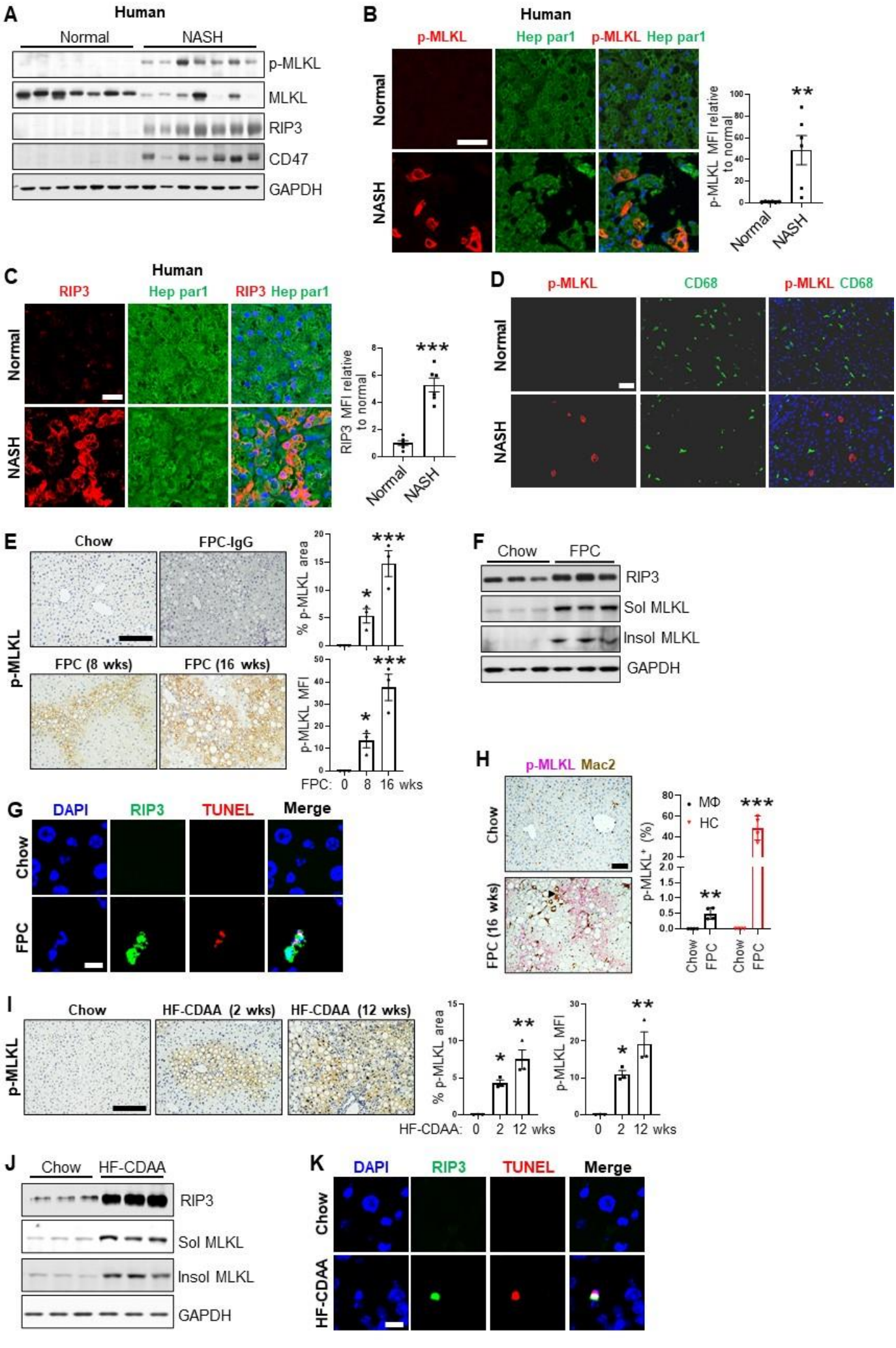
A
Human
Normal
NASH
p-MLKL
MLKL
RIP3
CD47
GAPDH
B
Human
p-MLKL
Hep par1
p-MLKL Hep par1
Normal
NASH
p-MLKL MFI relative to normal
**
Normal
NASH
C
Human
RIP3
Hep par1
RIP3 Hep par1
Normal
NASH
RIP3 MFI relative to normal
***
Normal
NASH
D
p-MLKL
CD68
p-MLKL CD68
Normal
NASH
E
Chow
FPC-IgG
FPC (8 wks)
FPC (16 wks)
p-MLKL
% p-MLKL area
p-MLKL MFI
***
*
FPC: 0 8 16 wks
F
Chow
FPC
RIP3
Sol MLKL
Insol MLKL
GAPDH
G
DAPI
RIP3
TUNEL
Merge
Chow
FPC
H
p-MLKL Mac2
Chow
FPC (16 wks)
MΦ
HC
p-MLKL+ (%)
***
**
Chow
FPC
Chow
FPC
I
Chow
HF-CDAA (2 wks)
HF-CDAA (12 wks)
p-MLKL
% p-MLKL area
p-MLKL MFI
**
*
HF-CDAA: 0 2 12 wks
0 2 12 wks
J
Chow
HF-CDAA
RIP3
Sol MLKL
Insol MLKL
GAPDH
K
DAPI
RIP3
TUNEL
Merge
Chow
HF-CDAA

Figure S1. Additional data documenting the accumulation of CD47$^+$ necroptotic hepatocytes in human and mouse NASH. (**A**) Western blots of p-MLKL, MLKL, RIP3, and CD47 in human normal and NASH liver specimens (n = 7/group). (**B**) Immunofluorescence staining of human normal and NASH liver sections using anti-p-MLKL (red) and anti-Hep par1 (hepatocyte marker, green). Scale bar, 50 μm. The data were quantified as relative mean fluorescent intensity (MFI) of p-MLKL relative to normal liver (**P < 0.01, n = 6/group). (**C**) Immunofluorescence staining of human normal and NASH liver sections using anti -RIP3 (red) and anti-Hep par1 (green). Scale bar, 25 μm. The data were quantified as RIP3 MFI relative to normal liver (***P < 0.001, n = 6/group). (**D**) Immunofluorescence staining of human normal and NASH liver sections using anti-p-MLKL (red) and anti-CD68 (macrophages; green). Scale bar, 50 μm. (**E**) Liver sections from male C57BL/6J mice fed the FPC NASH diet for 8 and 16 weeks or chow diet (0 FPC) were immunostained for p-MLKL (brown). The data were quantified as the percent p-MLKL-positive area and p-MLKL MFI relative to the 0-FPC group. (*P < 0.05, ***P < 0.001 vs. chow diet-fed mice, n = 3 mice/group). Scale bar, 50 μm. (**F**) Western blot of RIP3 and insoluble MLKL, with GAPDH as the loading control, in the livers of 16-week FPC diet-fed mice (n = 3 mice/group). **(G)** Immunofluorescence staining of liver from 16-week FPC diet-fed mice using anti-RIP3 (green) and TUNEL (red). Scale bar, 10 μm. (**H**) Liver sections from male C57BL/6J mice fed the FPC NASH diet or chow diet (0 FPC) for 16 weeks were immunostained for p-MLKL (Vibrant Red) and Mac2$^+$ macrophages (brown). The data were quantified as the percent p-MLKL$^+$Mac2$^+$ cells of total Mac2-positive cells. Arrowhead indicates an example of a p-MLKL$^+$Mac2$^+$ cell (**P < 0.01 vs. chow diet-fed mice, n = 4 mice/group). Scale bar, 50 μm. (**I**) Liver sections from male C57BL/6J mice fed the HF-CDAA diet for 2 and 12 weeks or chow diet (0 HF-CDAA) were immunostained for p-MLKL (brown). The data were quantified as the percent p-MLKL-positive area and p-MLKL MFI relative to the 0-FPC group. (*P < 0.05, **P < 0.01 vs. chow diet-fed mice, n = 3 mice/group). Scale bar, 50 μm. (**J**) Western blot of RIP3 and insoluble MLKL, with GAPDH as the loading control, in the livers of chow or 12-week HF-CDAA diet-fed mice (n = 3 mice/group). For all images, nuclei are stained with DAPI (blue). All data are presented as means ± SEM. (**K**) Immunofluorescence staining of liver from chow and 12-week HF-CDAA diet-fed mice using anti-RIP3 (green) and TUNEL (red). Scale bar, 10 μm.

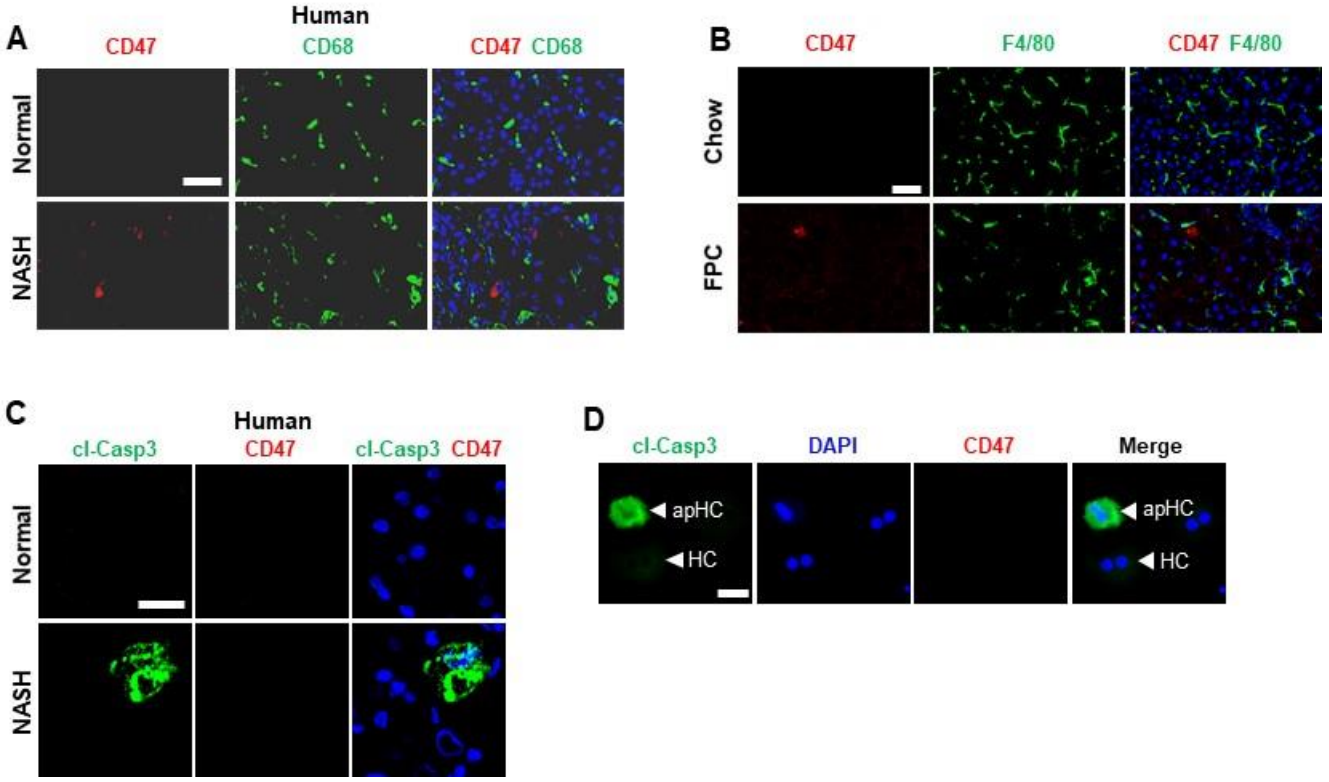

Figure S2. Additional data documenting the accumulation of CD47^{+} necroptotic hepatocytes in human and mouse NASH. (**A**) Immunofluorescence staining of human normal and NASH liver sections using anti-CD47 (red) and anti-CD68 (macrophages; green). Scale bar, 50 µm. (**B**) Immunofluorescence staining of liver from 16-week FPC diet-fed mice using anti-CD47 (red) and anti-F4/80 (macrophages; green). Scale bar, 50 µm. (**C**) Immunofluorescence staining of human normal and NASH liver sections using anti-cleaved-caspase 3 (cl-Casp3, green) and anti-CD47 (red). Scale bar, 25 µm. (**D**) Immunofluorescence staining of hepatocytes isolated from control and FasL (Jo2)-treated mice (hepatocytes [HC] and apoptotic hepatocytes [apHCs], respectively) using anti-cleaved-caspase 3 (cl-Casp3, green) and anti-CD47 (red). Scale bar, 25 µm. For all images, nuclei are stained with DAPI (blue).

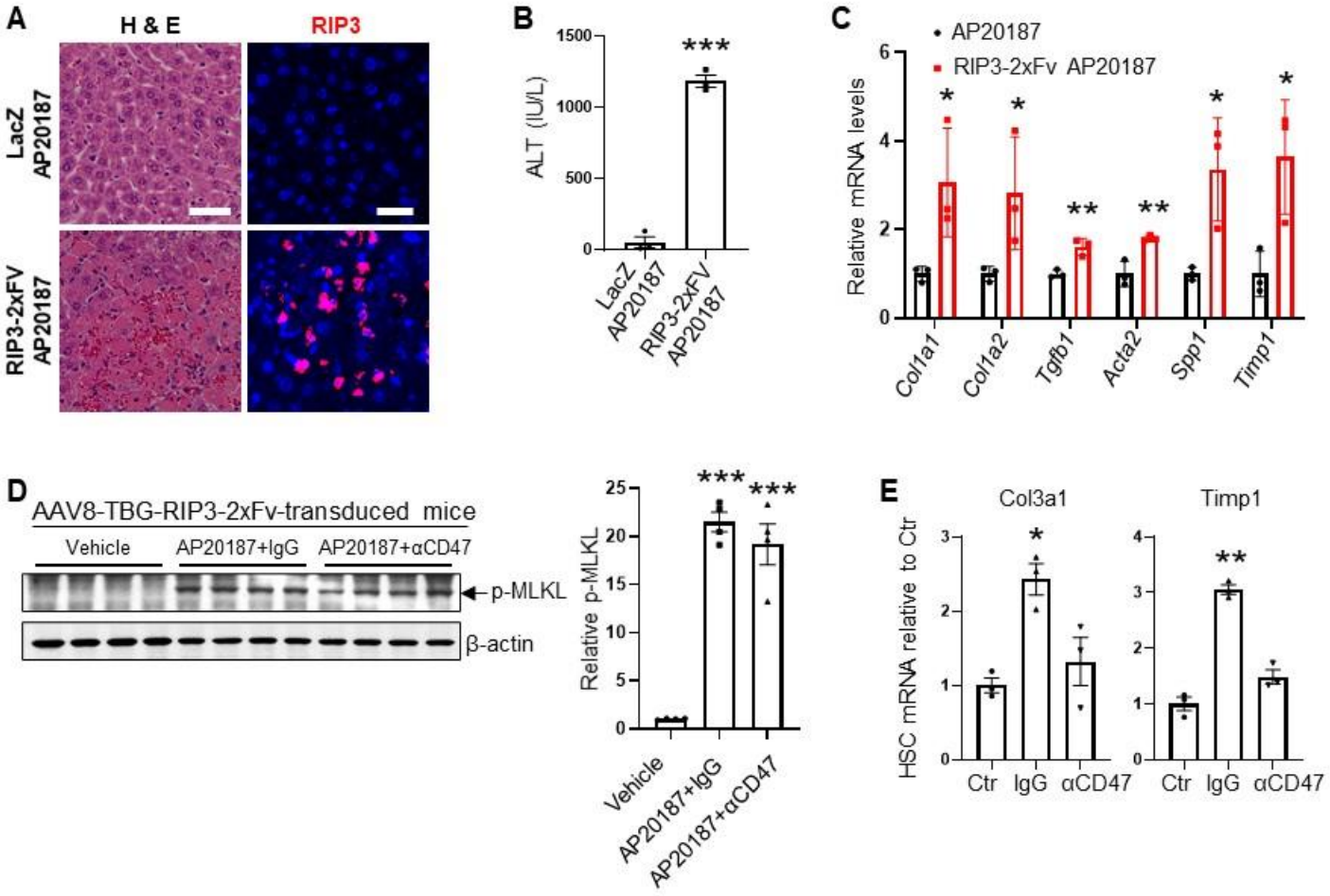

Figure S3. Additional data documenting that blocking CD47 increases necHC uptake by liver macrophages and blocks markers of HSC activation in a mouse model of hepatocyte necroptosis. (**A**) Livers from the AP20187-treated LacZ- and mRIP3-2xFV-transduced mice described in Fig. 2C were stained with H&E to show areas of liver hemorrhage and hepatocyte degeneration or with anti-RIP3 (red) and DAPI (blue). Scale bar, 25 μm. (**B-C**) The mice were also assayed for plasma ALT activity, and the livers were assayed for mRNAs related to HSC activation and liver fibrosis (**P* < 0.05, ***P* < 0.01, ****P* < 0.001; *n* = 3 mice/group). (**D**) Primary hepatocytes isolated from mice transduced with AAV8-TBG-mRIP3-2XFV were treated *ex vivo* with vehicle, AP20187 +IgG, or AP20187 + anti-CD47 and then assayed for p-MLKL and β-actin by immunoblot. (**E**) *Col3a1* and *Timp1* mRNA expression in control primary mouse HSCs (Ctr) or HSCs incubated with conditioned medium from co-cultures of macrophages and necHCs in the presence of IgG or anti-CD47 (**P* < 0.05, ***P* < 0.01; *n* = 3 biological replicates/group). All data are presented as means ± SEM.

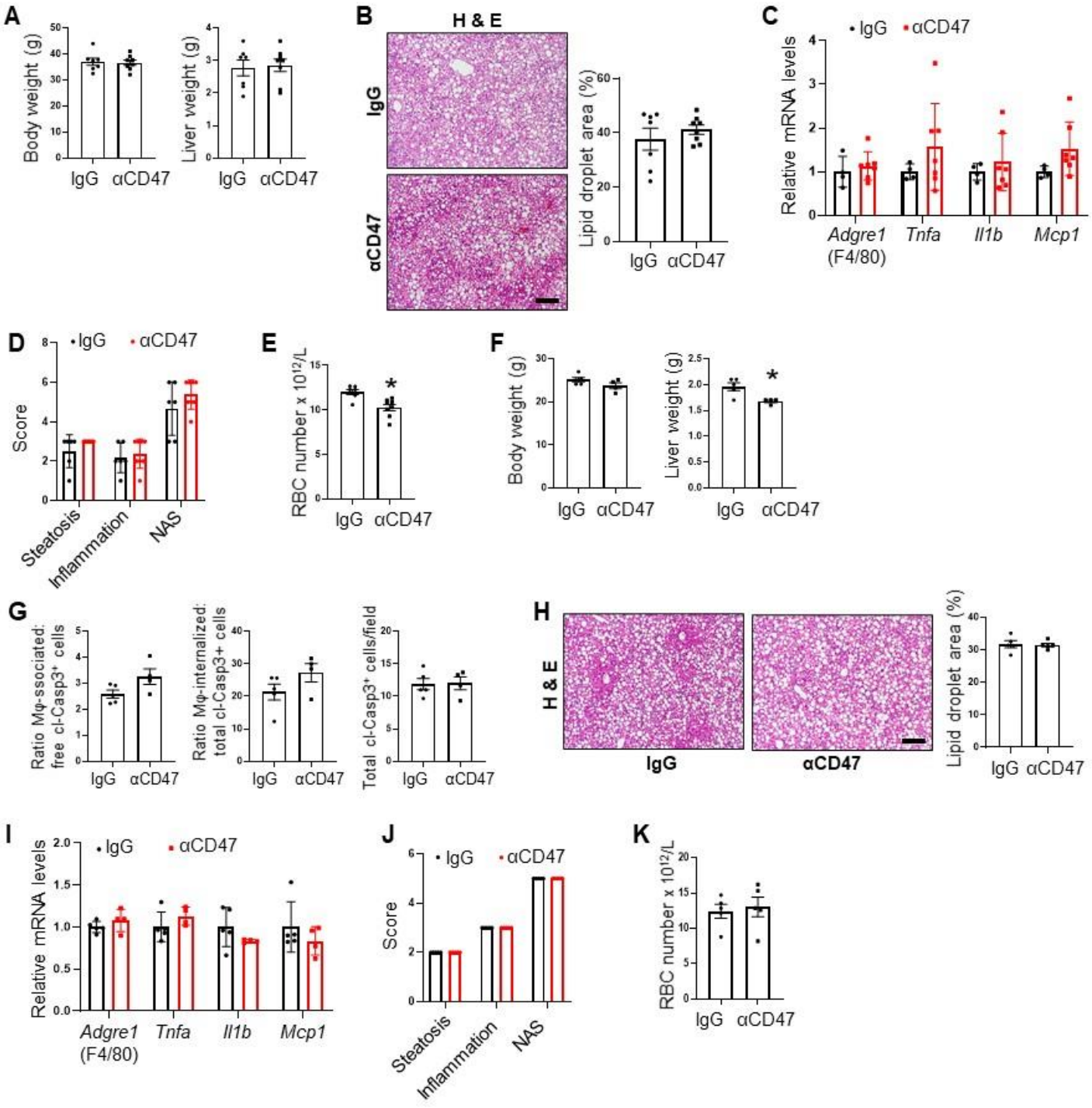

Figure S4. Additional characterization of NASH mice treated with anti-CD47. (**A-E**) The IgG- and anti-CD47-treated FPC-NASH mice described in Fig. 3 A-E (*n* = 4-7 mice/group) were assayed for the following: (**A**) Body and liver weight. (**B**) H & E staining of liver sections and lipid droplet area quantification. Scale bar, 250 µm. (**C**) mRNAs related to hepatic inflammation. (**D**) NAS score. **(E)** Red blood cell number (**P* < 0.05) **(F-K)** The IgG- or anti-CD47-treated HF-CDAA-NASH mice described in Fig. 4 F-K (*n* = 4-5 mice/group) were assayed for the following: (**F**) Body and liver weight. (**G**) Quantification of efferocytosis (ratio of macrophage-associated apoptotic hepatocytes to free apoptotic hepatocytes) in liver sections. (**H**) H & E staining of liver sections and lipid droplet area quantification. Scale bar, 250 µm. (**I**) mRNAs related to hepatic inflammation. (**J**) NAS score. (**K**) Red blood cell number. All data are presented as means ± SEM.

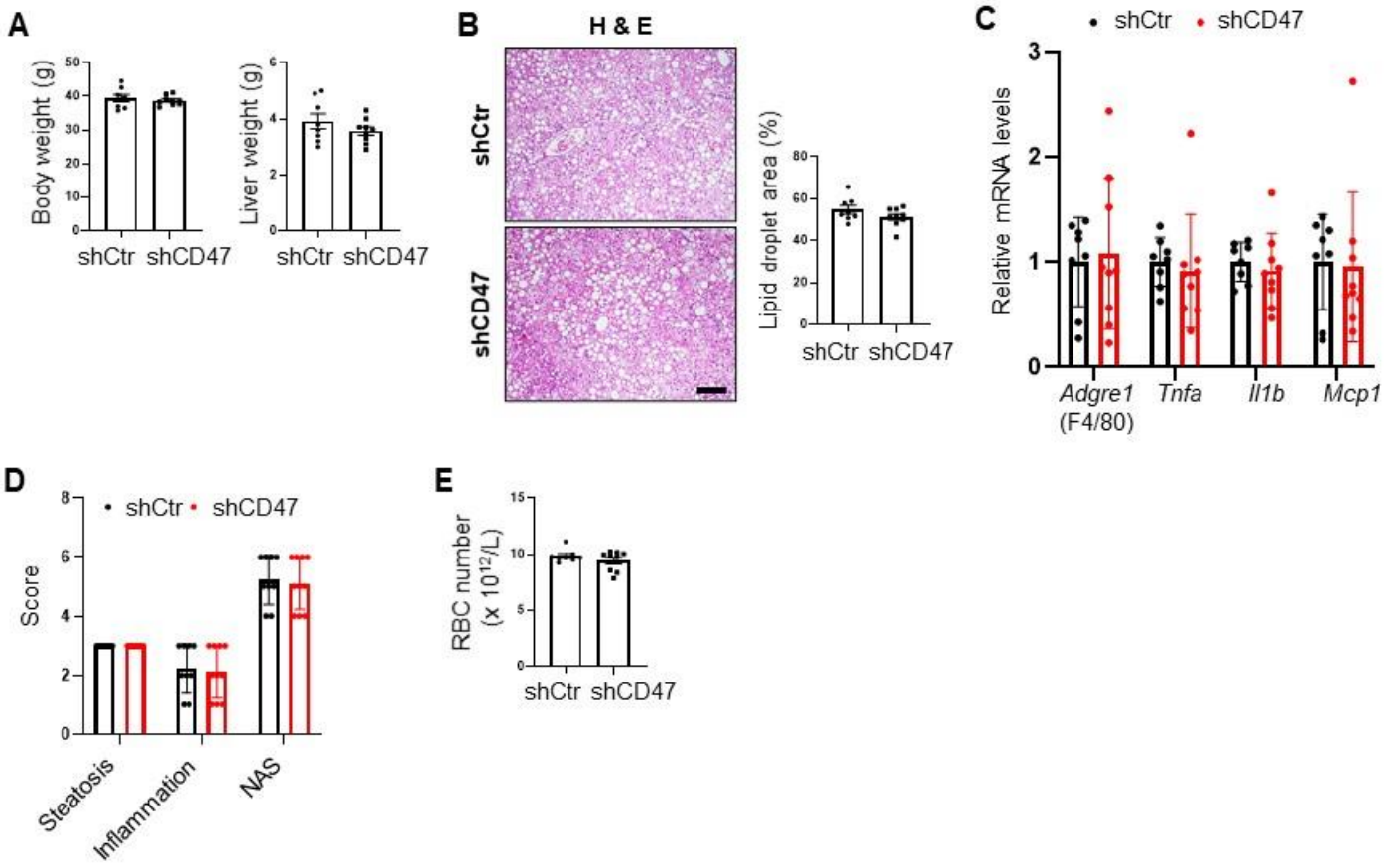

Figure S5. Additional characterization of NASH mice treated with AAV8-H1-shCD47. The FPC mice treated with AAV8-H1-shControl (shCtr) or AAV8-H1-shCD47 (shCD47) between weeks 8 and 16 (*n* = 8-10 mice/group) were assayed for the following: **(A)** Body and liver weight. (**B**) H & E staining of liver sections and lipid droplet area quantification. Scale bar, 250 μm. (**C**) mRNAs related to hepatic inflammation. **(D)** NAS score. (**E)** Red blood cell number. All data are presented as means ± SEM.

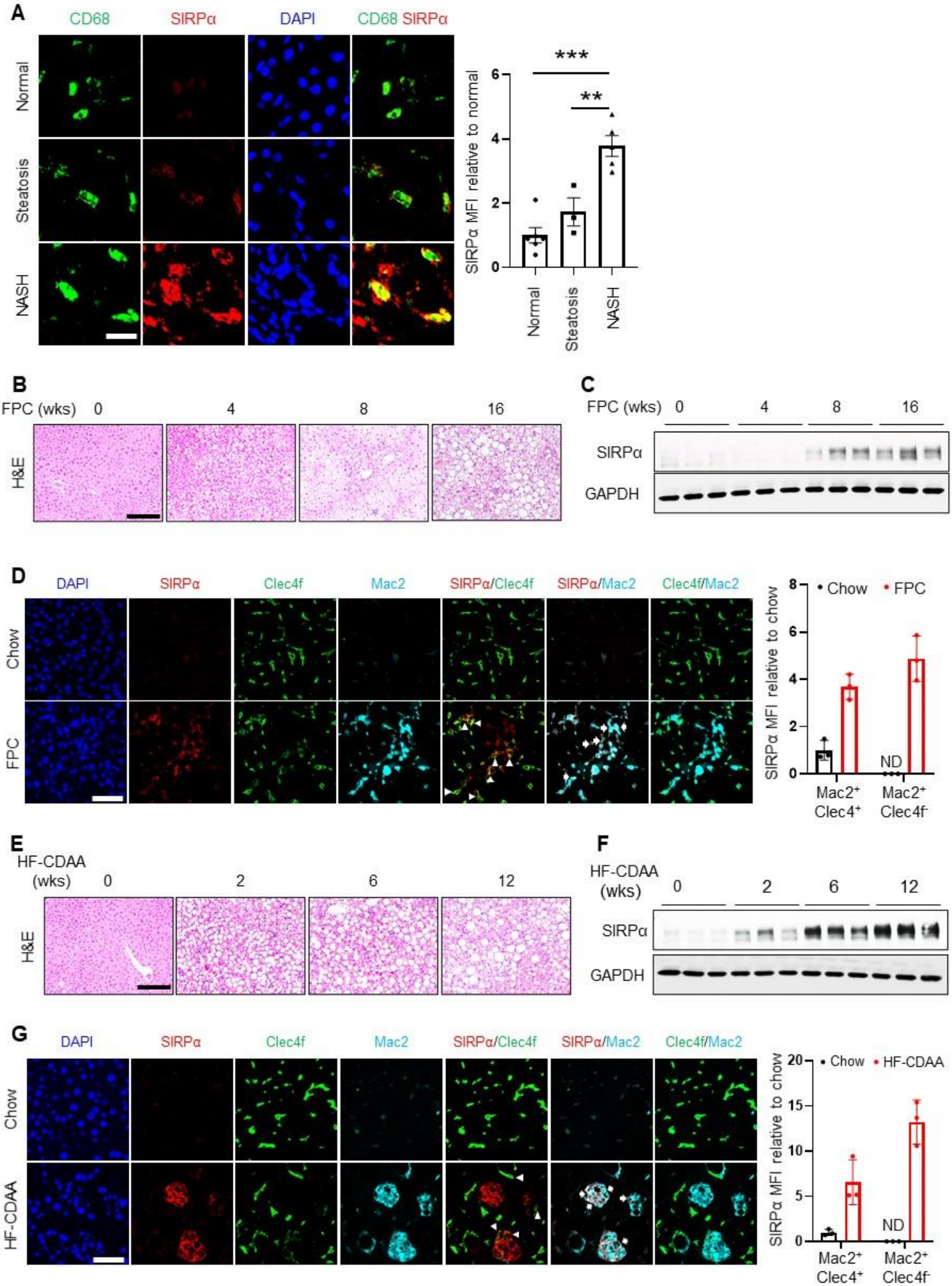
A
CD68
SIRPα
DAPI
CD68 SIRPα
Normal
Steatosis
NASH
SIRPα MFI relative to normal
***
**
Normal
Steatosis
NASH
B
FPC (wks) 0 4 8 16
H&E
C
FPC (wks) 0 4 8 16
SIRPα
GAPDH
D
DAPI
SIRPα
Clec4f
Mac2
SIRPα/Clec4f
SIRPα/Mac2
Clec4f/Mac2
Chow
FPC
SIRPα MFI relative to chow
Chow
FPC
ND
Mac2+ Clec4+
Mac2+ Clec4f-
E
HF-CDAA (wks) 0 2 6 12
H&E
F
HF-CDAA (wks) 0 2 6 12
SIRPα
GAPDH
G
DAPI
SIRPα
Clec4f
Mac2
SIRPα/Clec4f
SIRPα/Mac2
Clec4f/Mac2
Chow
HF-CDAA
SIRPα MFI relative to chow
Chow
HF-CDAA
ND
Mac2+ Clec4+
Mac2+ Clec4f-

Figure S6. Additional data related to SIRPα expression in human and mouse liver macrophages. (**A**) Immunofluorescence staining of normal, steatotic, and NASH human liver sections using anti-SIRPα (red) and anti-CD68 (green), with quantification of SIRPα MFI relative to the normal liver value (**$P < 0.01$,***$P < 0.001$). Scale bar, 25 μm. (**B**) H & E staining of liver sections of mice fed chow diet (0 weeks) or FPC diet for 4 weeks, 8 weeks, or 16 weeks. (**C**) Western blot of SIRPα, with GAPDH as the loading control, in the livers from panel B ($n = 3$ mice/group). (**D**) Liver sections from mice fed the FPC NASH diet or chow diet for 16 weeks were immunostained with anti-SIRPα (red), anti-Mac2 (all macrophages, cyan), and anti-Clec4f (liver resident KCs, green). Scale bar, 50 μm. Arrowheads show examples of liver resident KCs ($Mac2^+Clec4f^+$), and arrows show examples of infiltrated macrophages ($Mac2^+Clec4f^-$). (**E**) H & E staining of liver sections of mice fed chow diet (0 week) or the HF-CDAA diet for 2 weeks, 6 weeks, or 12 weeks. (**F**) Western blot of SIRPα, with GAPDH as the loading control, in the livers from panel E ($n = 3$ mice/group). (**G**) Liver sections from mice fed chow diet or the HF-CDAA diet for 8 weeks were immunostained with anti-SIRPα (red), anti-Mac2 (cyan), and anti-Clec4f (green). Scale bar, 50 μm. Arrowheads show examples of liver resident KCs ($Mac2^+Clec4f^+$), and arrows show examples of infiltrated macrophages ($Mac2^+Clec4f^-$).

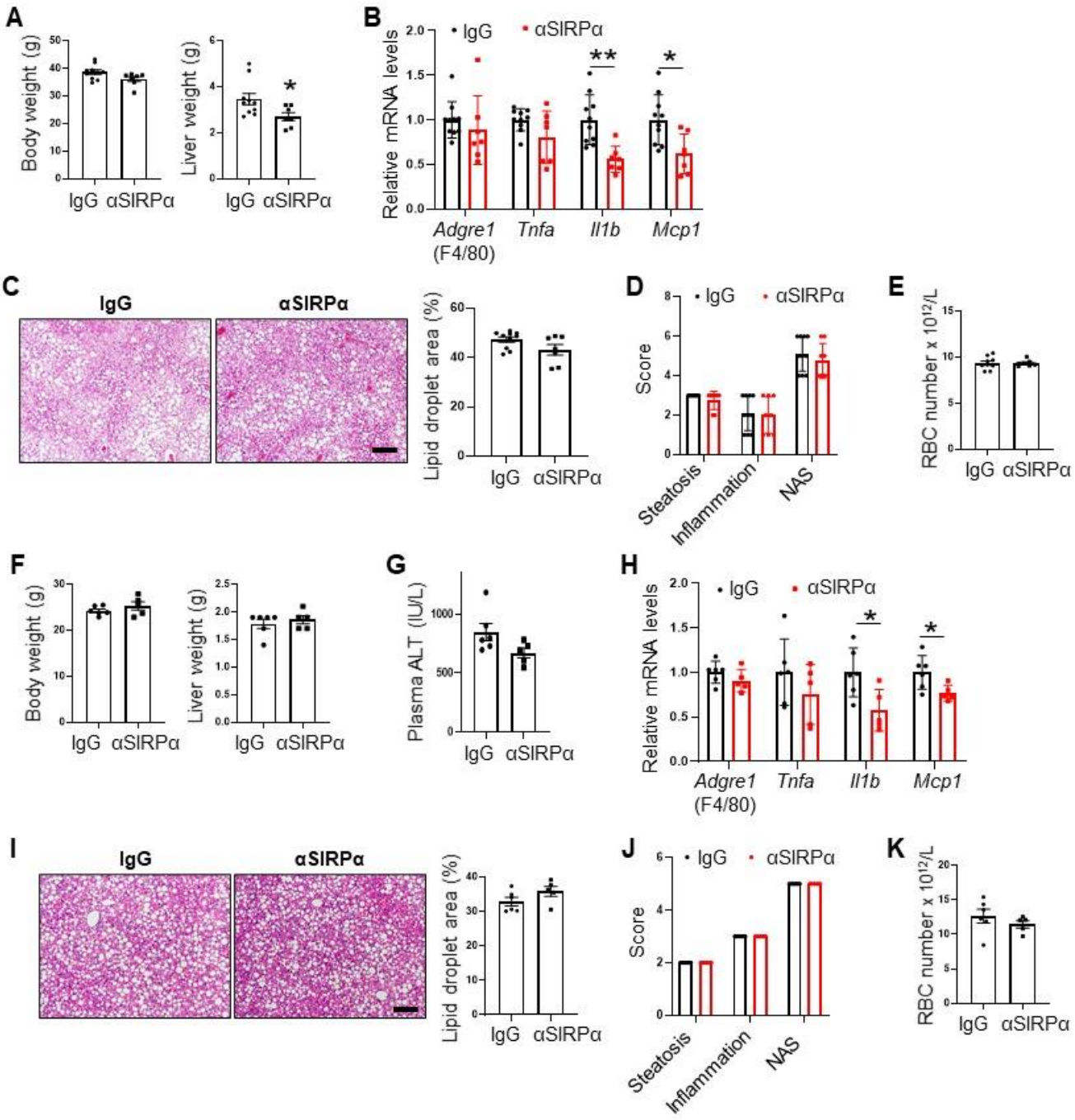

Figure S7. Additional characterization of NASH mice treated with anti-SIRPα. (**A-E**) The IgG- or anti-SIRPα-treated FPC-NASH mice described in Fig. 6 A-E (*n* = 7-10 mice/group) were assayed for the following: (**A**) Body and liver weight (**P* < 0.05). (**B**) mRNAs related to hepatic inflammation (**P* < 0.01, ***P* < 0.05) (**C**) H & E staining of liver sections and lipid droplet area quantification. Scale bar, 250 μm. (**D**) NAS score. (**E**) Red blood cell number. (**F-K**) The IgG- or anti-SIRPα-treated HF-CDAA-NASH mice described in Fig. 6 F-K (*n* = 5-6 mice/group) were assayed for the following: (**F**) Body and liver weight. (**G**) Plasma ALT activity (p=0.079). (**H**) mRNAs related to hepatic inflammation (**P* < 0.05). (**I**) H & E staining of liver sections and lipid droplet area quantification. Scale bar, 250 μm. (**J**) NAS score. (**K**) Red blood cell number. All data are presented as means ± SEM.

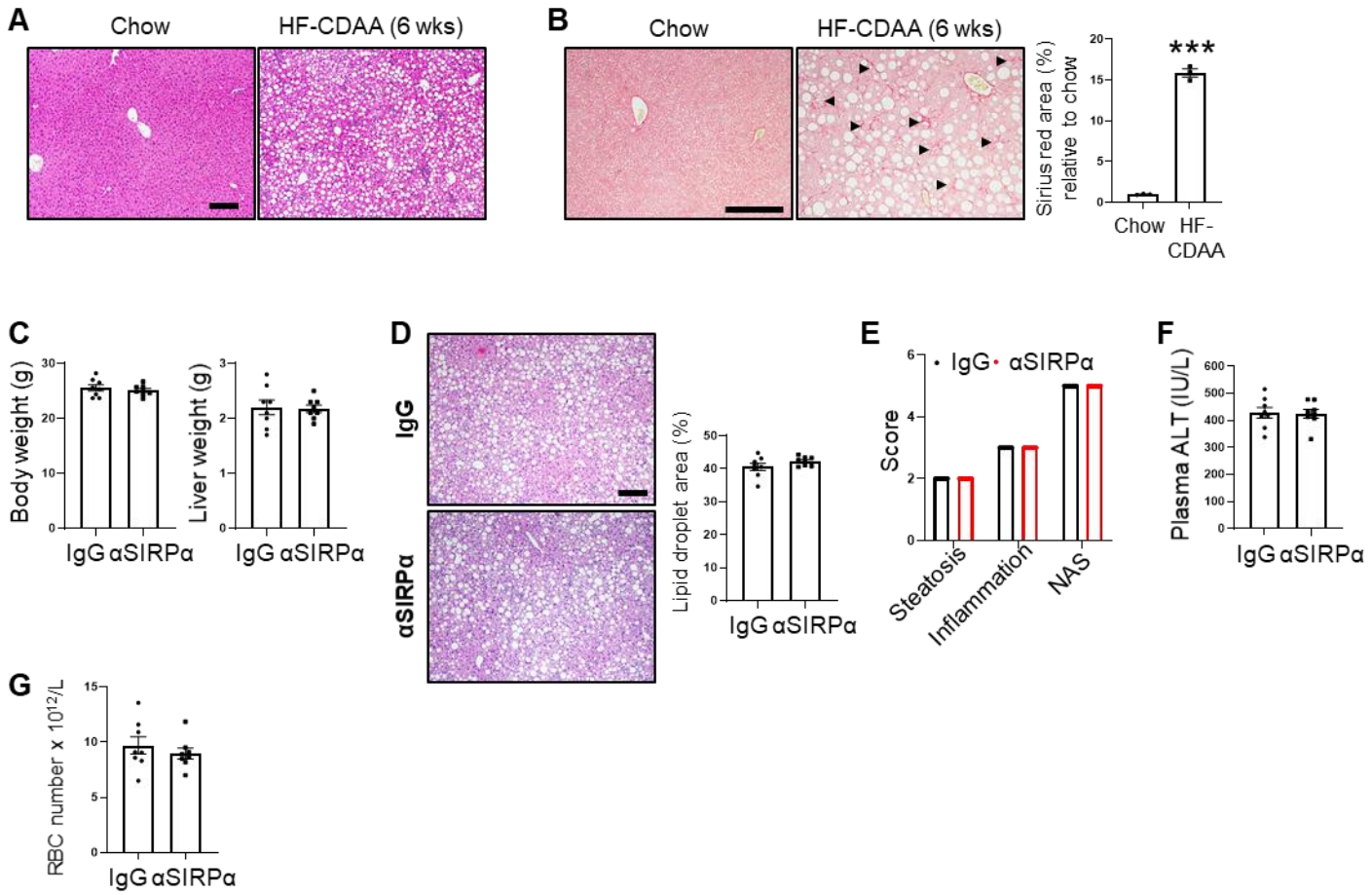

Figure S8. Additional characterization of mice with established NASH before and after anti-SIRPα treatment. Male C57BL/6J mice were fed the HF-CDAA NASH diet for 6 weeks and then harvested or continued on the diet for an additional 6 weeks and treated with IgG or anti-SIRPα. (*n*=8 mice/group). H&E staining (**A**) and quantification of Picrosirius red-positive area (arrowheads) (**B**) in livers after 6 weeks HF-CDAA diet feeding. Scale bar, 250 μm (*n* = 3 mice/group ***$P < 0.001$). Scale bar, 200 μm. (**C**) Body and liver weight. (**D**) H & E staining of liver sections and lipid droplet area quantification. Scale bar, 250 μm. (**E**) NAS score. (**F**) Plasma ALT activity. (**G**) Red blood cell number. All data are presented as means ± SEM.

Table S1. Pathology of human NASH liver samples. Related to Figure 1A, Figures 4A and 4B, and Figures. S1A-C.

ID	Age	Gender	Pathological diagnoses
1	57	Female	NASH cirrhosis
2	65	Female	Cirrhosis, mildly active, with extensive cholestasis. Occasional Mallory bodies.
3	56	Male	End stage cirrhotic liver disease. Negative for malignancy.
4	46	Female	Moderately active cirrhosis. No evidence of malignancy. Minimal current steatosis.
5	68	Male	Non-alcoholic steatohepatitis; cirrhosis, mixed macronodular and micronodular type. Minimal inflammatory activity, with minimal or no ongoing steatosis. No evidence of hepatocyte dysplasia or malignancy
6	56	Female	Advanced chronic liver disease (stage 4: "cirrhosis"). Marked fibrosis throughout the entire liver. The residual hepatocellular parenchyma shows abundant well-formed Mallory hyaline, consistent with advanced chronic liver disease from steatohepatitis.
7	68	Male	Cirrhosis with chronic hepatitis, mildly active, consistent with clinical history of non-alcoholic steatohepatitis. Minimal steatosis, macrovesicular type (<5%). Viable resection margins.
9	61	Female	Liver with mild portal inflammation, no significant steatosis or fibrosis
10	49	Male	Liver with mild steatosis, no fibrosis
11	51	Male	Liver with minimal non-specific changes
12	67	Female	Liver with no specific pathological changes
13	71	Female	Liver with minimal macrovesicular steatosis

Table S2. Mouse primer sequence used for qPCR.

Name	Sequence
Hprt F	TCAGTCAACGGGGGACATAAA
Hprt R	GGGGCTGTACTGCTTAACCAG
Col1a1 F	GCTCCTCTTAGGGGCCACT
Col1a1 R	CCACGTCTCACCATTGGGG
Col1a2 F	GTAACTTCGTGCCTAGCAACA
Col1a2 R	CCTTTGTCAGAATACTGAGCAGC
Col3a1 F	CTGTAACATGGAAACTGGGGAAA
Col3a1 R	CCATAGCTGAACTGAAAACCACC
Tgfb1 F	CTCCCGTGGCTTCTAGTGC
Tgfb1 R	GCCTTAGTTTGGACAGGATCTG
Acta2 F	ATGCTCCCAGGGCTGTTTTCCCAT
Acta2 R	GTGGTGCCAGATCTTTTCCATGTCG
Spp1 F	CTGACCCATCTCAGAAGCAGAATCT
Spp1 R	TCCATGTGGTCATGGCTTTCATTGG
Timp1 F	GCAACTCGGACCTGGTCATAA
Timp1 R	CGGCCCGTGATGAGAAACT
F4/80 F	ACCACAATACCTACATGCACC
F4/80 R	AAGCAGGCGAGGAAAAGATAG
Tnfa F	CTTCTGTCTACTGAACTTCGGG
Tnfa R	CAGGCTTGTCACTCGAATTTTG
Il1b F	CAACCAACAAGTGATATTCTCCATG
Il1b R	GATCCACACTCTCCAGCTGCA
Mcp1 F	TTAAAAACCTGGATCGGAACCAA
Mcp1 R	GCATTAGCTTCAGATTTACGGGT

Hprt, hypoxanthine guanine phosphoribosyl transferase; *Col1a1*, collagen type I alpha 1; *Col1a2*, collagen type I alpha 2; *Col3a1*, collagen, type III alpha 1; *Tgfb1*, transforming growth factor, beta 1; *Acta2*, actin alpha 2, smooth muscle, aorta; *Spp1*, secreted phosphoprotein 1; *Timp1*, TIMP metallopeptidase inhibitor 1; *F4/80*, adhesion G protein-coupled receptor E1; *Tnfa*, tumor necrosis factor-α ; *Il1b*, interleukin 1 beta; *Mcp1*, monocyte chemoattractant protein-1.